Monolayer to Bilayer Structural Transition in Confined Pyrrolidinium-Based Ionic Liquids

ARTICLE *in* JOURNAL OF PHYSICAL CHEMISTRY LETTERS · FEBRUARY 2013

Impact Factor: 7.46 · DOI: 10.1021/jz301965d

7 AUTHORS, INCLUDING:

Nitya Nand Gosvami
University of Pennsylvania
39 PUBLICATIONS **448** CITATIONS
SEE PROFILE

Peter Licence
University of Nottingham
117 PUBLICATIONS **3,732** CITATIONS
SEE PROFILE

THE JOURNAL OF PHYSICAL CHEMISTRY Letters

Letter

pubs.acs.org/JPCL

Monolayer to Bilayer Structural Transition in Confined Pyrrolidinium-Based Ionic Liquids

Alexander M. Smith,[†] Kevin R. J. Lovelock,[‡] Nitya Nand Gosvami,[§] Peter Licence,[∥] Andrew Dolan,[‡] Tom Welton,[‡] and Susan Perkin*[,†]

[†]Department of Chemistry, Physical and Theoretical Chemistry Laboratory, University of Oxford, South Parks Road, Oxford OX1 3QZ, United Kingdom

[‡]Department of Chemistry, Imperial College London, London SW7 2AZ, United Kingdom

[§]Department of Mechanical Engineering and Applied Mechanics, University of Pennsylvania, 220 South 33rd Street, Philadelphia, Pennsylvania 19104, United States

[∥]School of Chemistry, The University of Nottingham, University Park, Nottingham NG7 2RD, United Kingdom

ABSTRACT: Ionic liquids can be intricately nanostructured in the bulk and at interfaces resulting from a delicate interplay between interionic and surface forces. Here we report the structuring of a series of dialkylpyrrolidinium-based ionic liquids induced by confinement. The ionic liquids containing cations with shorter alkyl chain substituents form alternating cation−anion monolayer structures on confinement to a thin film, whereas a cation with a longer alkyl chain substituent leads to bilayer formation. The crossover from monolayer to bilayer structure occurs between chain lengths of n = 8 and 10 for these pyrrolidinium-based ionic liquids. The bilayer structure for n = 10 involves full interdigitation of the alkyl chains; this is in contrast with previous observations for imidazolium-based ionic liquids. The results are pertinent to these liquids' application as electrolytes, where the electrolyte is confined inside the pores of a nanoporous electrode, for example, in devices such as supercapacitors or batteries.

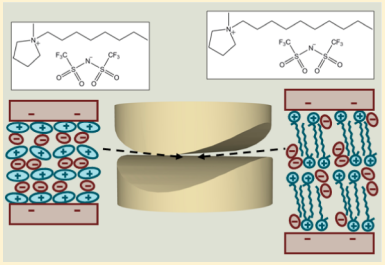

SECTION: Surfaces, Interfaces, Porous Materials, and Catalysis

Salts that are in their liquid state at room temperature − called ionic liquids − are finding applications as electrolytes in energy storage devices[1] and for electrodeposition,[2] as solvents for nanoparticle stabilization[3] and as lubricants.[4] These applications depend critically on how the ionic liquid behaves when confined to films or pores, for example, lubricant films or nanoporous carbon electrodes in supercapacitors.[5,6] This has driven recent interest in how ionic liquids behave at solid interfaces and in confined geometries, which turns out to be remarkably complex compared to standard molecular liquids.[6−9] In the bulk, ionic liquids often display mesostructural ordering with segregated regions of polar and nonpolar domains:[10−13] this domain formation and self-assembly is driven by a combination of Coulombic, van der Waals, and hydrogen-bonding interactions. At the interface with a solid surface, there are additional driving forces for liquid ordering such as screening of surface charges and template effects. The entropic cost of ordering is also reduced due to confinement. The result can be alternating layers of cations and anions extending several ion layers (corresponding to distances up to ∼10 nm) when confined between charged solid surfaces[14−17] and even extending away from a single charged surface.[18−20]

Pyrrolidinium-based ionic liquids are of particular interest for electrical applications due to their high thermal stability, very low volatility,[21] nonflammability, and their wide "electrochemical window": the range of voltages at which the liquid remains stable is wider for dialkylpyrrolidinium-based ionic liquids than for dialkylimidazolium-based ionic liquids and enormously greater than for aqueous electrolytes.[22−24] Pyrrolidinium-based ionic liquids have been studied both by experiments[18,25,26] and simulations[27] at solid interfaces before, but here is the first study of their confinement between two extended surfaces. We show, for a homologous series of 1-alkyl-1-methylpyrrolidinium bis[(trifluoromethane)sulfonyl]imide ionic liquids, $[C_nC_1Pyrr][NTf_2]$ with n = 4, 6, 8, and 10 (see Figure 1 for chemical structures), that layered ion structures are induced by confinement of the liquid to films between two macroscopic, atomically smooth charged surfaces. A transition between two different layering structures occurs as the alkyl chain length on the cation increases: ionic liquids containing shorter alkyl chain substituents on the cation align into alternating cation−anion monolayers, whereas ionic liquids containing longer alkyl chain substituents lead to bilayer formation. The bilayers formed for these pyrrolidinium cations have an interdigitated structure, qualitatively different from the toe-to-toe orientation observed for analogous 1-alkyl-3-methylimidazolium ionic liquids.[28] The results lead to an understanding of mesostructure in pyrrolidinium-based ionic

Received: November 28, 2012
Accepted: January 3, 2013
Published: January 3, 2013

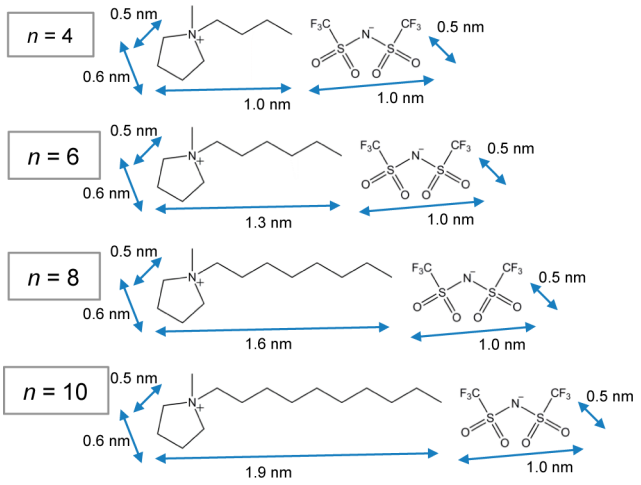

Figure 1. Chemical structures and approximate ion dimensions calculated from van der Waals radii of the ionic liquids investigated in this study: $[C_nC_1Pyrr][NTf_2]$, with n = 4, 6, 8, and 10.

liquids with direct implications for their application as electrolytes, solvents, and lubricants.

Using a surface force balance (SFB), the normal interaction force, F_N, between atomically smooth mica sheets was measured across films of ionic liquid, with submolecular resolution in surface separation, D. The technique and detailed experimental procedures have been described elsewhere.[29] In brief, two back-silvered mica pieces of 1.5 to 2.5 μm thickness are glued to two cylindrical silica lenses and mounted in the apparatus in a crossed-cylinder configuration. In this arrangement, the mica surfaces have a point of closest approach, geometrically equivalent to a sphere near a flat surface. White-light multiple beam interferometry is used to determine D by means of constructive interference fringes of equal chromatic order.[30] The deflection of a horizontal leaf spring is measured via interferometry to determine F_N, with resolution better than 10^{-7} N. Forces are normalized by the local radius of curvature, R, of the glued mica surfaces ($R \approx 1$ cm): F_N/R is proportional to the interaction energy per unit area between parallel plates and so allows quantitative comparison between different contacts and different experiments.

All ionic liquids investigated in this study were prepared at the University of Nottingham and Imperial College London using modifications of existing literature methods.[31,32] The ionic liquids were characterized using NMR spectroscopy, electrospray ionization MS, and Karl Fischer titration. The structures of the ionic liquids investigated in this study are shown in Figure 1. We find that an exceptional level of ionic liquid purity is required for successful SFB experiments because the presence of even minute amounts of surface active contamination can dramatically affect the reproducibility of the measured forces. The ionic liquids were not treated by column chromatography because this has been shown to introduce particulate impurities.[33] All ionic liquids were thoroughly washed with water, then dried in vacuo (10^{-2} mbar, 70 °C) for 24 h prior to injection into the SFB apparatus (see details below). Karl Fischer titration showed the water levels were <50 ppm prior to injection into the SFB apparatus.

After calibration of the mica–mica contact in dry air to determine mica thickness, a droplet of the ionic liquid (~100 μL) was injected between the surfaces. This process is likely to introduce a small amount of water, giving an estimated water content of <200 ppm. Care was taken to keep the atmosphere dry inside the SFB chamber by purging with dry, reduced hydrocarbon nitrogen before sealing, and a vial containing P_2O_5 was placed inside the apparatus to absorb residual water vapor. It is known from control experiments that additional humidity or water content would lead to expunging of the oscillatory forces reported here. We observe no change in forces during the first 5–10 h of each experiment, indicating no substantial increase in water content in the ionic liquid samples during this time.

Force profiles for $[C_nC_1Pyrr][NTf_2]$, with n = 4, 6, 8, and 10, are reported in Figure 2 and show results from two to six different experiments (each employing different mica pieces) for each ionic liquid. The force profiles show both positive (repulsive) and negative (attractive) F_N as D is decreased; that is, oscillations in F_N with respect to D are observed. Such oscillatory force profiles are observed for ionic liquids[14−17,28] and nonpolar liquids[34,35] when the liquid is structured in ordered layers between two surfaces. The oscillatory forces are caused by the sequential squeeze-out of liquid layers, observed as repulsive walls at specific D values which match a stable liquid configuration (an integral number of layers), and attraction at intermediate thicknesses corresponding to unstable films. Retraction of the surfaces from any point on the force profile leads to a jump-apart of the surfaces from the nearest adhesive minimum (marked as filled triangles in Figure 2). These outward jumps are observed when using spring deflection to measure attractive forces: on retracting the surfaces at a particular stable film thickness D, the spring will extend until the attractive force balances the elastic restoring force. Once the gradient of the attractive force dF/dD exceeds the spring constant, K, the surfaces jump apart to large separations. This jump distance multiplied by K yields the force of adhesion (using Hooke's law); in this way, F_N values at the adhesive minima are measured independently of the remainder of the force profile and provide additional evidence for the layer structure. Figure 3 highlights these measurements of the adhesive force at each stable film thickness and for each ionic liquid: Figure 3a shows how the layering film thickness and adhesion values are similar for n = 4, 6, and 8, whereas Figure 3b shows the different values for n = 10. The positions of the repulsive walls in the oscillatory force profile, and, in particular, the location of these energy minima, can be used to determine the layering structure of the confined film, as we next describe.

The oscillatory force profiles obtained for $[C_nC_1Pyrr][NTf_2]$ with n = 4, 6, and 8 are similar: each shows four distinct energy minima at similar D values for the three ionic liquids. The repeat distances are indicative of cation–anion layer structure in the films, based on electrostatic and geometric arguments, as follows. To preserve electroneutrality of the confined ionic liquid, each maximum in the force law must represent squeeze-out of an equal number of cations and anions. The difference in separation between the repulsive walls (ΔD in the inset tables) is close to the thickness of a single cation–anion layer (monolayer), with the hydrocarbon tails in the plane of the surfaces, suggesting that the stable film structures are composed of stacks of cation–anion monolayers. Electrostatic arguments (as well as simulation studies[7,36]) suggest that the layers are arranged as alternating cation–anion layers. This interpretation of the oscillatory forces is in line with previous studies of other ionic liquids at surfaces and in confined films.[15−17,19,28,37]

dx.doi.org/10.1021/jz301965d | J. Phys. Chem. Lett. 2013, 4, 378−382

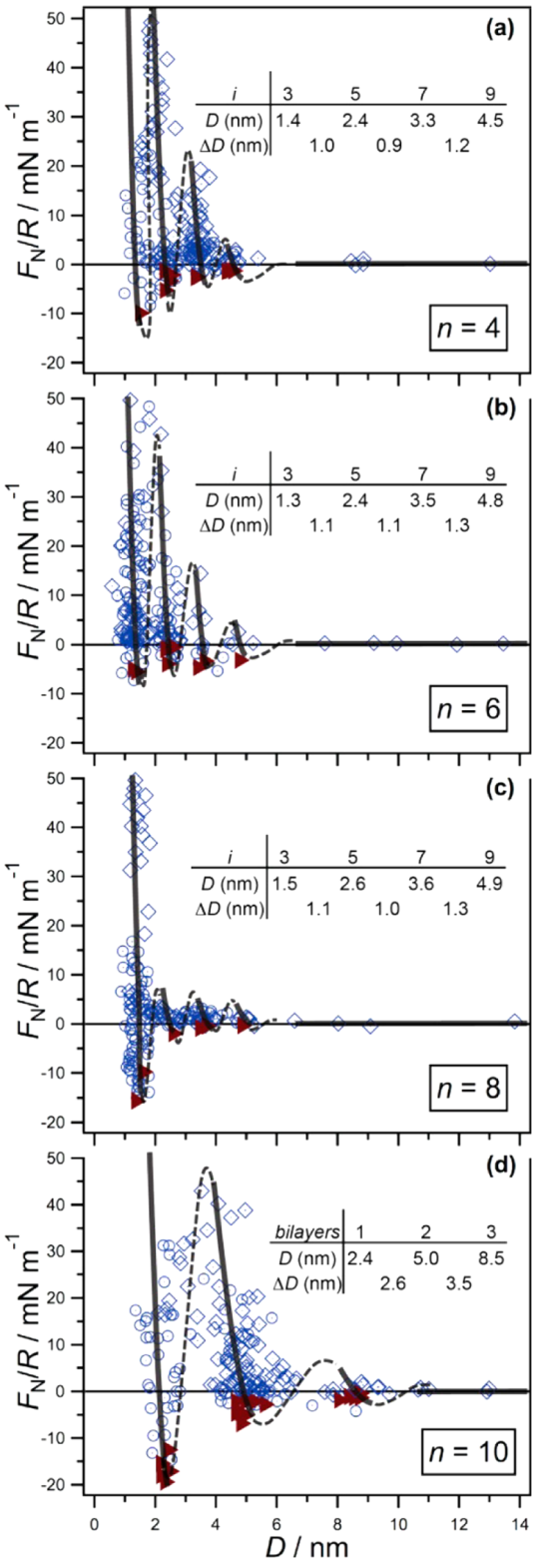

Figure 2. Measured force, F_N, between two mica surfaces (normalized by radius of curvature, R) as a function of film thickness, D, for (a) $[C_4C_1Pyrr][[NTf_2]$, (b) $[C_6C_1Pyrr][NTf_2]$, (c) $[C_8C_1Pyrr][NTf_2]$, and (d) $[C_{10}C_1Pyrr][NTf_2]$. Forces were measured from $D \approx 200$ nm, but only the region between 0 and 14 nm, where nonzero forces were observed, is shown. Open diamonds indicate points measured on approach of the surfaces while open circles indicate data measured on retraction of the surfaces. Filled triangles indicate points measured from the jump-apart of the surfaces from an adhesive minimum. The lines are a guide to the eye to show the oscillatory nature of the forces,

Figure 2. continued

with solid lines through measured regions and dashed lines through the regions inaccessible to measurement due to the jump-in from the previous energy barrier. The inset tables show mean values of D for each wall in the oscillatory profile, and ΔD is the distance between adjacent walls.

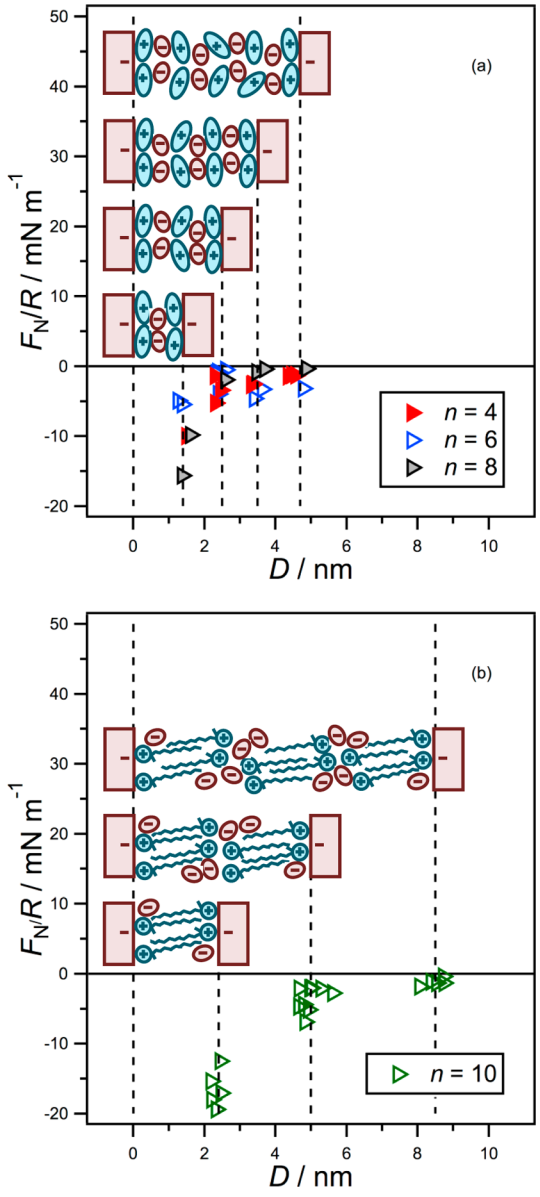

Figure 3. Points measured from the jump-apart of the surfaces from an adhesive minimum for: (a) $[C_nC_1Pyrr][NTf_2]$ where n = 4, 6, and 8 and (b) $[C_{10}C_1Pyrr][NTf_2]$ and dashed lines showing the mean value for each energy minimum. The shorter chain ionic liquids show close similarity of the stable film thicknesses, and the interpretation of how these relate to layered film structures is indicated in the inset cartoons. The larger distances between stable film thicknesses for n = 10 ionic liquid leads to the interpretation of interdigitated bilayers (as explained in the text). Although these schematics show 100% cations or anions in each layer, this is a simplification for clarity and in fact the layers decrease in purity with distance extending from each surface.

For these three liquids, the closest minimum is at $D \approx 1.4$ nm. This thinnest film corresponds to three ion layers (i = 3) due to the requirement for excess cations in the film to

dx.doi.org/10.1021/jz301965d | J. Phys. Chem. Lett. 2013, 4, 378−382

neutralize the negative mica charge:[20] next to each negatively charged mica surface lies an electrostatically bound layer of cations, with an intermediate layer consisting mostly of anions. Similarly, for larger D at 2.5, 3.5, and 4.7 nm, there are stable configurations corresponding to 5, 7, and 9 ion layers (i = 5, 7 and 9), respectively, as depicted in Figure 3a. The film could not be squeezed down to a single cation layer (i = 1) for these ionic liquids under the forces applied here. The similar layer repeat distances for these three liquids of different cation alkyl chain lengths suggest that the cations lie with their alkyl chains parallel to the surface. However, the significantly weaker force magnitudes exhibited by $[C_8C_1Pyrr][NTf_2]$ could indicate the alkyl chains starting to cause disorder in the interfacial structure (Figure 2c), a hint as to the structuring transition observed between n = 8 and 10.

The situation is more complex for $[C_{10}C_1Pyrr][NTf_2]$, which exhibits strong oscillatory forces, indicating layered structure in the film but with repeat distances too large to be explained simply by squeeze-out of a single cation−anion layer. Repeating the experiment with samples from different synthesis batches gave identical results, strongly suggesting that the ionic liquids are highly pure and that the different interfacial structure is not an effect of contamination. To explain the observed larger D values we note that ionic liquids with more amphiphilic cations (i.e., containing longer alkyl chains) can self-assemble into structures which collect together the polar and nonpolar moieties. In confined films, this was previously observed for 1-alkyl-3-methylimidazolium-based analogues,[28] where cations were found to form a toe-to-toe bilayer structure once the alkyl chain length reached six carbons in length. Our results suggest that such bilayer formation also occurs for $[C_{10}C_1Pyrr][NTf_2]$ confined to films between mica surfaces. Comparing the layer thickness (Figure 2d) with the ion dimensions, it is clear that there must be significant, if not full, interdigitation of the decyl chains in its bilayer structure. Thus we propose that for this $[C_{10}C_1Pyrr][NTf_2]$ ionic liquid three stable confinement-induced layer configurations are observed consisting of one, two, or three layers of interdigitated cation bilayers, shown schematically in Figure 3b. We note with interest the common feature of a crossover from monolayers to bilayers observed for imidazolium-based and pyrrolidinium-based ionic liquids yet with differing "critical" (crossover) chain length and different bilayer architecture for these two classes of ionic liquids; the molecular origins of these differences will be discussed in a future publication.

These observed layering structures in confined films differ from the sponge-like and percolating structures observed in bulk ionic liquids. The difference is due to a combination of the ion−surface interactions, the symmetry breaking effect of the surface, and the entropy loss due to confinement. The bulk structure of pyrrolidinium-based ionic liquids also has increased ordering on the mesoscale as alkyl chain length increases,[38] with the observation of a first sharp diffraction peak when n > 8. This transition in bulk structure is likely to be due to similar interionic forces as the structuring transition reported here, although in the bulk liquid structure the transition is gradual with the peak growing as n increases, compared with the discontinuous change reported here for a confined liquid film. The suggested interdigitated chain structure for the bilayers fits well with the data observed here and bears notable resemblance with the bulk crystal structures; however, we do not rule out the presence of other conformations such as crumpled or tilted alkyl chains in the bilayers.

In summary, we have used an SFB to demonstrate oscillatory force behavior between mica surfaces across a homologous series of pyrrolidinium-based ionic liquids, allowing us to detect and determine the dimensions of layered structures in the liquid film. We find that a transition between two different interfacial structures occurs upon increasing the alkyl chain length of the cation. As observed in previous experiments, the ionic liquids containing cations with a shorter alkyl chain form alternating layers of cations and anions when confined to thin films, whereas a longer chain cation leads to bilayer formation. In this case, the bilayers are greatly interdigitated due to the shape of the pyrrolidinium headgroup and the need for the ions to fill space most effectively. These results have direct implications for their application in solvating polar or nonpolar solutes, determining molecular mechanisms of boundary lubrication, and for their use as electrolytes confined to narrow pores in energy devices. Pyrrolidinium-based ionic liquids are particularly attractive for these electrochemical applications due to their wide electrochemical window and chemical stability compared with other ionic liquids and conventional solvents.

AUTHOR INFORMATION

Corresponding Author

*E-mail: susan.perkin@chem.ox.ac.uk.

Notes

The authors declare no competing financial interest.

ACKNOWLEDGMENTS

This work was supported by The Leverhulme Trust (F/07 134/DK and F/07 134/DN), Taiho Kogyo Tribology Research Foundation, Weizmann UK, Infineum UK, and the EPSRC (EP/J015202/1). We thank Men Shuang and Dan Mitchell for help with ionic liquid synthesis.

REFERENCES

(1) Armand, M.; Endres, F.; MacFarlane, D. R.; Ohno, H.; Scrosati, B. Ionic-Liquid Materials for the Electrochemical Challenges of the Future. *Nat. Mater.* **2009**, *8*, 621−629.

(2) *Electrodeposition from Ionic Liquids*; Endres, F., Abbott, A. P., MacFarlane, D. R., Eds.; Wiley-VCH: Weinheim, Germany, 2008.

(3) Dupont, J.; Scholten, J. D. On the Structural and Surface Properties of Transition-Metal Nanoparticles in Ionic Liquids. *Chem. Soc. Rev.* **2010**, *39*, 1780−1804.

(4) Zhou, F.; Liang, Y.; Liu, W. Ionic Liquid Lubricants: Designed Chemistry for Engineering Applications. *Chem. Soc. Rev.* **2009**, *38*, 2590−2599.

(5) Chmiola, J.; Yushin, G.; Gogotsi, Y.; Portet, C.; Simon, P.; Taberna, P. L. Anomalous Increase in Carbon Capacitance at Pore Sizes Less Than 1 Nanometer. *Science* **2006**, *313*, 1760−1763.

(6) Merlet, C.; Rotenberg, B.; Madden, P. A.; Taberna, P.-L.; Simon, P.; Gogotsi, Y.; Salanne, M. On the Molecular Origin of Supercapacitance in Nanoporous Carbon Electrodes. *Nat. Mater.* **2012**, *11*, 306−310.

(7) Kornyshev, A. A. Double-Layer in Ionic Liquids: Paradigm Change? *J. Phys. Chem. B* **2007**, *111*, 5545−5557.

(8) Pensado, A. S.; Pádua, A. A. H. Solvation and Stabilization of Metallic Nanoparticles in Ionic Liquids. *Angew. Chem., Int. Ed.* **2011**, *50*, 8683−8687.

(9) Perkin, S. Ionic Liquids in Confined Geometries. *Phys. Chem. Chem. Phys.* **2012**, *14*, 5052−5062.

(10) Wang, Y. T.; Voth, G. A. Unique Spatial Heterogeneity in Ionic Liquids. *J. Am. Chem. Soc.* **2005**, *127*, 12192−12193.

(11) Canongia Lopes, J. N. A.; Pádua, A. A. H. Nanostructural Organization in Ionic Liquids. *J. Phys. Chem. B* **2006**, *110*, 3330−3335.

(12) Triolo, A.; Russina, O.; Bleif, H.-J.; Di Cola, E. Nanoscale Segregation in Room Temperature Ionic Liquids. *J. Phys. Chem. B* **2007**, *111*, 4641−4644.
(13) Bhargava, B. L.; Devane, R.; Klein, M. L.; Balasubramanian, S. Nanoscale Organization in Room Temperature Ionic Liquids: A Coarse Grained Molecular Dynamics Simulation Study. *Soft Matter* **2007**, *3*, 1395−1400.
(14) Horn, R. G.; Evans, D. F.; Ninham, B. W. Double-Layer and Solvation Forces Measured in a Molten-Salt and Its Mixtures with Water. *J. Phys. Chem.* **1988**, *92*, 3531−3537.
(15) Perkin, S.; Albrecht, T.; Klein, J. Layering and Shear Properties of an Ionic Liquid, 1-Ethyl-3-Methylimidazolium Ethylsulfate, Confined to Nano-Films between Mica Surfaces. *Phys. Chem. Chem. Phys.* **2010**, *12*, 1243−1247.
(16) Bou-Malham, I.; Bureau, L. Nanoconfined Ionic Liquids: Effect of Surface Charges on Flow and Molecular Layering. *Soft Matter* **2010**, *6*, 4062−4065.
(17) Ueno, K.; Kasuya, M.; Watanabe, M.; Mizukami, M.; Kurihara, K. Resonance Shear Measurement of Nanoconfined Ionic Liquids. *Phys. Chem. Chem. Phys.* **2010**, *12*, 4066−4071.
(18) Mezger, M.; Schröder, H.; Reichert, H.; Schramm, S.; Okasinski, J. S.; Schöder, S.; Honkimäki, V.; Deutsch, M.; Ocko, B. M.; Ralston, J.; Rohwerder, M.; Stratmann, M.; Dosch, H. Molecular Layering of Fluorinated Ionic Liquids at a Charged Sapphire (0001). *Surf. Sci.* **2008**, *322*, 424−428.
(19) Atkin, R.; Warr, G. G. Structure in Confined Room-Temperature Ionic Liquids. *J. Phys. Chem. C* **2007**, *111*, 5162−5168.
(20) Zhou, H.; Rouha, M.; Feng, G.; Lee, S. S.; Docherty, H.; Fenter, P.; Cummings, P. T.; Fulvio, P. F.; Dai, S.; McDonough, J.; Presser, V.; Gogotsi, Y. Nanoscale Perturbations of Room Temperature Ionic Liquid Structure at Charged and Uncharged Interfaces. *ACS Nano* **2012**, *6*, 9818−9827.
(21) Deyko, A.; Lovelock, K. R. J.; Corfield, J.-A.; Taylor, A. W.; Gooden, P. N.; Villar-Garcia, I. J.; Licence, P.; Jones, R. G.; Krasovskiy, V. G.; Chernikova, E. A.; Kustov, L. M. Measuring and Predicting Delta H-Vap(298) Values of Ionic Liquids. *Phys. Chem. Chem. Phys.* **2009**, *11*, 8544−8555.
(22) Macfarlane, D. R.; Forsyth, M.; Howlett, P. C.; Pringle, J. M.; Sun, J.; Annat, G.; Neil, W.; Izgorodina, E. I. Ionic Liquids in Electrochemical Devices and Processes: Managing Interfacial Electrochemistry. *Acc. Chem. Res.* **2007**, *40*, 1165−1173.
(23) Wibowo, R.; Aldous, L.; Rogers, E. I.; Jones, S. E. W.; Compton, R. G. A Study of the Na/Na+ Redox Couple in Some Room Temperature Ionic Liquids. *J. Phys. Chem. C* **2010**, *114*, 3618−3626.
(24) *Electrochemical Aspects of Ionic Liquids*; Ohno, H., Ed.; Wiley-Interscience: Hoboken, NJ, 2011.
(25) Hayes, R.; El Abedin, S. Z.; Atkin, R. Pronounced Structure in Confined Aprotic Room-Temperature Ionic Liquids. *J. Phys. Chem. B* **2009**, *113*, 7049−7052.
(26) Atkin, R.; El Abedin, S. Z.; Hayes, R.; Gasparotto, L. H. S.; Borisenko, N.; Endres, F. AFM and STM Studies on the Surface Interaction of [Bmp]Tfsa and [Emim]Tfsa Ionic Liquids with Au(111). *J. Phys. Chem. C* **2009**, *113*, 13266−13272.
(27) Vatamanu, J.; Borodin, O.; Smith, G. D. Molecular Insights into the Potential and Temperature Dependences of the Differential Capacitance of a Room-Temperature Ionic Liquid at Graphite Electrodes. *J. Am. Chem. Soc.* **2010**, *132*, 14825−14833.
(28) Perkin, S.; Crowhurst, L.; Niedermeyer, H.; Welton, T.; Smith, A. M.; Gosvami, N. N. Self-Assembly in the Electrical Double Layer of Ionic Liquids. *Chem. Commun.* **2011**, *47*, 6572−6574.
(29) Perkin, S.; Chai, L.; Kampf, N.; Raviv, U.; Briscoe, W.; Dunlop, I.; Titmuss, S.; Seo, M.; Kumacheva, E.; Klein, J. Forces between Mica Surfaces, Prepared in Different Ways, across Aqueous and Non-aqueous Liquids Confined to Molecularly Thin Films. *Langmuir* **2006**, *22*, 6142−6152.
(30) Israelachvili, J. Thin-Film Studies Using Multiple-Beam Interferometry. *J. Colloid Interface Sci.* **1973**, *44*, 259−272.
(31) Men, S.; Lovelock, K. R. J.; Licence, P. X-Ray Photoelectron Spectroscopy of Pyrrolidinium-Based Ionic Liquids: Cation-Anion Interactions and a Comparison to Imidazolium-Based Analogues. *Phys. Chem. Chem. Phys.* **2011**, *13*, 15244−15255.
(32) Ab Rani, M. A.; Brant, A.; Crowhurst, L.; Dolan, A.; Lui, M.; Hassan, N. H.; Hallett, J. P.; Hunt, P. A.; Niedermeyer, H.; Perez-Arlandis, J. M.; Schrems, M.; Welton, T.; Wilding, R. Understanding the Polarity of Ionic Liquids. *Phys. Chem. Chem. Phys.* **2011**, *13*, 16831−16840.
(33) Endres, F.; El Abedin, S. Z.; Borissenko, N. Probing Lithium and Alumina Impurities in Air- and Water Stable Ionic Liquids by Cyclic Voltammetry and in Situ Scanning Tunneling Microscopy. *Z. Phys. Chem.* **2006**, *220*, 1377−1394.
(34) Horn, R. G.; Israelachvili, J. N. Direct Measurement of Structural Forces between 2 Surfaces in a Non-Polar Liquid. *J. Chem. Phys.* **1981**, *75*, 1400−1411.
(35) Klein, J.; Kumacheva, E. Simple Liquids Confined to Molecularly Thin Layers. I. Confinement-Induced Liquid-to-Solid Phase Transitions. *J. Chem. Phys.* **1998**, *108*, 6996−7009.
(36) Lynden-Bell, R. M.; Frolov, A. I.; Fedorov, M. V. Electrode Screening by Ionic Liquids. *Phys. Chem. Chem. Phys.* **2012**, *14*, 2693−2701.
(37) Zhang, X.; Zhong, Y.-X.; Yan, J.-W.; Su, Y.-Z.; Zhang, M.; Mao, B.-W. Probing Double Layer Structures of Au (111)-Bmipf6 Ionic Liquid Interfaces from Potential-Dependent AFM Force Curves. *Chem. Commun.* **2012**, *48*, 582−584.
(38) Santos, C. S.; Murthy, N. S.; Baker, G. A.; Castner, E. W. Communication: X-ray Scattering from Ionic Liquids with Pyrrolidinium Cations. *J. Chem. Phys.* **2011**, *134*, 121101.